Determination of v-Mos-Catalyzed Phosphorylation Sites and Autophosphorylation Sites on MAP Kinase Kinase by ESI/MS†

Katheryn A. Resing,‡,§ Sam J. Mansour,‡,|| April S. Hermann,‡,§ Richard S. Johnson,⊥ Julian M. Candia,‡,§ Kenji Fukasawa,# George F. Vande Woude,# and Natalie G. Ahn*,‡,§

Department of Chemistry and Biochemistry, Department of Molecular, Cellular and Developmental Biology, and Howard Hughes Medical Institute, University of Colorado, Boulder, Colorado 80309, Department of Biochemistry, University of Washington, Seattle, Washington 98195, and ABL Basic Research Program, National Cancer Institute, Frederick, Maryland 21702

Received September 13, 1994; Revised Manuscript Received December 6, 1994⊗

ABSTRACT: MAP kinase kinase (MAPKK), a key component of the MAP kinase cascade, is activated through phosphorylation by several protein kinases, including the oncogene v-Mos and its cellular counterpart, c-Mos. The v-Mos-catalyzed phosphorylation sites on recombinant MAPKK1 were identified by electrospray ionization mass spectrometry as S_{218} and S_{222}, located within a sequence that aligns with the T loop structure of cAMP-dependent protein kinase; these are the same as the Raf-1 phosphorylation sites identified previously [Alessi, D. R., et al. (1994) *EMBO J. 13*, 1610−1619]. Phosphorylation of these sites was kinetically ordered, with S_{222} preferred over S_{218}. Intramolecular autophosphorylation of MAPKK occurred at several residues and was increased upon the stimulation of MAPKK activity by v-Mos. Major autophosphorylation sites were residues S_{298} and Y_{300}. Minor autophosphorylation sites included T_{23}, S_{299}, S_{218}, and either S_{24} or S_{25}. Sequence similarities were noted between MAPKK autophosphorylation sites and exogenous phosphorylation sites on MAP kinase. Phosphorylation of *either* S_{218} or S_{222} was sufficient for partial MAPKK activation by Mos, and phosphorylation of S_{222} alone was sufficient for autophosphorylation at S_{298} and Y_{300}. Mass spectral analysis was also performed on MAPKK1 purified from rabbit skeletal muscle. The peptide containing S_{218} and S_{222} was observed in only a singly phosphorylated form, and the peptide containing S_{298}, S_{299}, and Y_{300} was observed in multiply phosphorylated forms, suggesting that MAPKK is only partially phosphorylated within the T loop but significantly modified in the autophosphorylation loop under physiological conditions.

Extracellular stimuli in various cell types activate signal transduction pathways that often converge on the MAP kinase cascade, which consists of MAP kinase (MAPK,[1] also known as extracellular regulated kinase or ERK) and its activator, MAP kinase kinase (MAPKK, also known as MAP/ERK kinase or MEK) (Nishida & Gotoh, 1993). Activation of MAPK requires phosphorylation by MAPKK on both threonine and tyrosine residues within the sequence $FLT_{183}EY_{185}VA$ [illustrated for the MAPK isoform, ERK2 (Payne et al., 1991)]. MAPKK itself is a substrate for phosphorylation and activation by any of several upstream kinases, including Raf-1 (Kyriakis et al., 1992; Dent et al., 1992; Howe et al., 1992), Mos (Posada et al., 1993; Shibuya & Ruderman, 1993; Nebreda & Hunt, 1993), STE11 and byr2 (Zhou et al., 1993; Neiman & Herskowitz, 1994; Neiman et al., 1993), and MEK kinase (Lange-Carter et al., 1993). Of these, Raf-1 and MEK kinase are regulated by Ras-dependent and -independent signaling pathways that regulate growth and differentiation in mammalian cells. STE11 and byr2 are MEK kinase homologs that function in mating signal transduction pathways in *Saccharomyces cerevisiae* and *Schizosaccharomyces pombe*, respectively. Mos is a protein kinase selectively expressed in germ cells that leads to the stimulation of MAPKK and MAPK, which then function during meiotic cell division. To understand how MAPKK and MAPK may be activated by separate and diverse pathways, we characterized the phosphorylation of MAPKK by Mos, taking advantage of recent developments in mass spectrometry (MS) that facilitate the analysis of protein posttranslational modifications.

Electrospray ionization (Fenn et al., 1989) has been introduced as a novel way to volatilize peptides for mass analysis. When directly coupled to a chromatography system (LC/MS), on-line analysis of column eluates can be accomplished without the need for peptide purification. The use of two quadrupole mass analyzers allows the selection of parent ions of specific mass to charge ratio (*m/z*) in the first quadrupole, which is then fragmented by collision-induced dissociation (Cooks, 1978). A series of fragment

† Supported by NIH Grants GM48521 (N.G.A.), AR39730 (K.A.R.), and RR05543 (to Kenneth A. Walsh), the Royalty Research Fund (R.S.J.), the National Cancer Institute, DHHS, under Contract N01-CO-7410I with ABL (G.F.V.W.), and the G. Harold and Leila Y. Mathers Charitable Foundation (K.F.). N.G.A. is a Searle Scholar.

* Author to whom correspondence should be addressed: Department of Chemistry and Biochemistry, Campus Box 215, University of Colorado, Boulder, CO 80309.

‡ Department of Chemistry and Biochemistry, University of Colorado.

§ Howard Hughes Medical Institute, University of Colorado.

|| Department of Molecular, Cellular and Developmental Biology, University of Colorado.

⊥ University of Washington.

National Cancer Institute.

⊗ Abstract published in *Advance ACS Abstracts,* February 1, 1995.

[1] Abbreviations: ERK, extracellular signal-regulated kinase; ESI, electrospray ionization; LC, liquid chromatography; MAPKK, MAP kinase kinase; MAPK, MAP kinase; MS, mass spectrometry; MS/MS, tandem mass spectrometry; *m/z*, mass to charge ratio; SDS−PAGE, sodium dodecyl sulfate−polyacrylamide gel electrophoresis.

0006-2960/95/0434-2610$09.00/0

ions that provide sequence information is detected in the second quadrupole mass analyzer. This process, known as tandem mass spectrometry or MS/MS (McLafferty, 1983), can be applied to peptides present in mixtures or in eluates from HPLC (LC/MS/MS).

In this study, ESI/MS was used to analyze sites of phosphorylation on recombinant MAPKK activated by Mos and on purified MAPKK. Several MAPKK autophosphorylation sites were also identified, some of which are present under physiological conditions. The technique discriminated between heterogeneously phosphorylated intermediates, yielding new insights into the mechanism of activation of MAPKK.

MATERIALS AND METHODS

Preparation and Phosphorylation of Recombinant MAPKK. Recombinant human MAPKK1 was expressed in *Escherichia coli*, and soluble protein was purified as described (Mansour et al., 1994b). The resulting fusion protein contained a 5 kDa addition with the amino acid sequence MRGSHHHHHHGMASMTGGQQMGRDLYDDDDKDRWGSGGVGSALPGSK at the amino terminus. Site-directed mutagenesis was performed using the Mutagene phagemid in vitro mutagenesis kit (Bio-Rad) to generate amino acid substitutions indicated in the Results. The entire wild-type sequence and all mutations were confirmed by dideoxynucleotide sequencing of double-stranded DNA.

Swiss 3T3 cells were stably transformed with v-*mos* (Tx-7; Fukasawa et al., 1994), and confluent monolayers were treated with 0.1 μM phorbol 12-myristate 13-acetate for 10 min at 37 °C. Immunoprecipitates of v-Mos were prepared from cell extracts as described (Mansour et al., 1994a). MAPKK activation reactions (50 μL) were performed by incubating the resin-bound v-Mos with wild-type or mutant MAPKK (0.25 μg) at 30 °C in 50 mM Hepes (pH 7.4), 0.01% TX100, 0.1 mM [γ-^{32}P]ATP (300 Ci/mol), 10 mM $MgCl_2$, and 1 mM dithiothreitol. At various times, the resin was removed by centrifugation, and 35 μL of the supernatant was added to 2.5 μg (5 μL) of catalytically inactive ERK2-(K52R) and incubated for 5 min before termination and separation by SDS−PAGE/autoradiography. For mass spectrometry, resin-bound v-Mos was incubated with wild-type or mutant MAPKK (8 μg) at 30 °C in 50 mM Hepes (pH 7.4), 0.01% TX100, 4 mM ATP, 15 mM $MgCl_2$, and 2 mM dithiothreitol (90 μL). After the resin was removed, phosphorylated MAPKK was alkylated with 4-vinylpyridine as described (Mansour et al., 1994b). Polymers from detergent, resin, and 4-vinylpyridine were removed by acetone precipitation of MAPKK, and pellets were redissolved in 1.6 M urea, 2 mM $CaCl_2$, and 0.2 M Tris (pH 8.0) and digested with *N*-tosyl-L-phenylalanyl chloromethyl ketone-treated trypsin (5% (w/w), Worthington) and endoproteinase LysC (5% (w/w), Wako) for 3 h at 37 °C. In some instances, samples were further digested with endoproteinase AspN (5% (w/w), Boehringer Mannheim) for 3 h at 37 °C. To estimate phosphorylation stoichiometries, parallel reactions were carried out in the presence of [γ-^{32}P]ATP (30 Ci/mol) and separated by SDS−PAGE, and label incorporated into MAPKK was determined by scintillation counting.

Preparation of Rabbit Muscle MAPKK. MAPKK was purified from frozen rabbit skeletal muscle (Pel Freeze) as described (Seger et al., 1992a), except that batch adsorption to Whatman DE52 cellulose (25 mM β-glycerophosphate (pH 8.3), 12 mM Tris-HCl, 2 mM EDTA, 2 mM EGTA, 50 μM sodium orthovanadate, 1 mM benzamidine, 5 μg/mL leupeptin, 5 μg/mL aprotinin, 1 μg/mL pepstatin A, and 1 mM phenylmethanesulfonyl fluoride) was added as the first step and 0.1% (v/v) β-mercaptoethanol was added to all column buffers. Reversed phase fast performance liquid chromatography (Pharmacia ProRPC HR10/5 developed with 0.1% TFA/acetonitrile) was added as the last step of purification. Acetonitrile/TFA was removed by lyophilization to approximately 8% of the original volume. The concentrated sample was then diluted with an equal volume of 1 M Tris/2 mM $CaCl_2$ (pH 8) containing 10 ng of trypsin. After digestion for 3 h at 37 °C, formic acid was added to a final concentration of 5%, and samples were analyzed by LC/MS.

Mass Spectral Analyses. Mass determinations were carried out as previously described (Mansour et al., 1994b; Resing et al., 1993) on an API-III triple quadrupole mass spectrometer (Sciex, Thornhill, Ontario, Canada) equipped with a nebulization-assisted electrospray source and a high-pressure collision cell. The ion spray needle was held at a potential of 4.6 kV with an orifice voltage of 75 V. Mass spectra were acquired at unit resolution, scanning from 400 to 1700 Da/e with a dwell time of 0.5 ms and a 0.15−0.22 Da/e step size for recombinant or rabbit skeletal muscle MAPKK, respectively. Digests were analyzed by reversed phase HPLC (Applied Biosystems Model 140B) directly coupled to the mass spectrometer (LC/MS), using metal-free injector and connections. Peptide separations were carried out on 500 μm × 20 cm (flow rate, 20 μL/min) or 250 μm × 15 cm (flow rate, 4 μL/min, achieved using a precolumn splitter) fused silica capillary columns, packed with POROS 120R (PerSeptive Systems) or Vydac C18 or HP C18 (Hewlett-Packard) resin, respectively. Columns were packed as described (Davis & Lee, 1992), except that Teflon filter paper was used as the frit material. Columns were equilibrated in 0.1% formic acid or 0.05% TFA and developed with a gradient into acetonitrile in the same buffer.

MS/MS was performed on-line as peptides eluted from the capillary column, selecting individual peptide ions for collision-induced dissociation in the high-pressure collision cell (LC/MS/MS). Precursor ions were accelerated to a kinetic energy of 28 eV and collisionally activated with argon at a thickness of (2.5−4.0) × 10^{14} atoms/cm^3. With some of the smaller peptides (less than or equal to 10 amino acids in length), sequences were determined by collision-induced dissociation prior to entry into the first quadrupole mass analyzer by raising the orifice voltage to 95 V (Katta et al., 1991). Analysis of LC/MS and LC/MS/MS data, including quantitation of peptide signal intensity, was carried out using software provided by Sciex, which allowed the quantitation of peptide signal intensities by the integration of peak areas [for example, see Figures 3 and 4 in Mansour et al. (1994b)]. Figures were prepared by importing data into Sigmaplot graphics software. Individual peptides typically eluted with peak widths of 20−60 s; therefore, step sizes (ranging from 0.15 to 0.22 Da/e) and dwell times (ranging from 0.7 to 0.9 ms) for LC/MS/MS were adjusted to produce 6 s scan times. In some cases, peaks of closely eluting contaminants were subtracted from the spectra of analyzed ions. Fragment ions produced were "b" and "y" types [nomenclature as in Biemann (1990)], representing cleavage between the amide nitrogen and the carbonyl of the peptide backbone. Internal

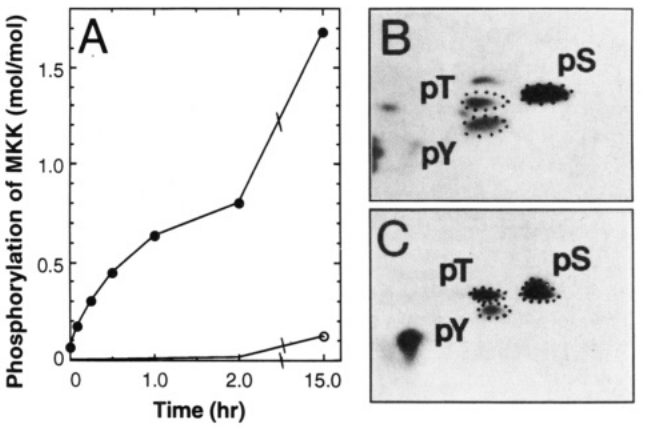

FIGURE 1: v-Mos phosphorylation and autophosphorylation of MAPKK. (A) Time course of MAPKK (0.5 μg) phosphorylation, incubated for varying times at 30 °C in the presence (●) and absence (○) of immunoprecipitated v-Mos, as indicated in Materials and Methods. (B) Phosphoamino acid analysis of MAPKK after phosphorylation with v-Mos for 3 h. (C) Phosphoamino acid analysis of MAPKK after autophosphorylation for 3 h. Exposure times of the autoradiographs in (B) and (C) were 1 and 15 h, respectively. Abbreviations used are as follows: pS, phosphoserine; pT, phosphothreonine; pY, phosphotyrosine.

fragment ions resulting from two such cleavages were often observed, as were "a" type ions, which represent the loss of CO from the b ions. In some cases, doubly and triply charged fragment ions were observed (referred to as b^{2+}, b^{3+}, and y^{2+}, which correspond to $(b+1H)^{2+}$, $(b+2H)^{3+}$, and $(y+1H)^{2+}$ in the Biemann nomenclature, respectively).

Thin-Layer Plate Phosphopeptide Mapping and Phosphoamino Acid Analysis. MAPKK was autophosphorylated or phosphorylated by v-Mos in the presence of [γ-^{32}P]ATP (100 μM, 1000 Ci/mol) and separated from reaction components by SDS−PAGE. Tryptic/endoproteinase LysC maps were carried out on silica thin-layer plates with electrophoresis in the first dimension [formic acid/acetic acid/water (2.5:7.8:89.7)] and chromatography in the second dimension [isobutyric acid/*n*-butanol/pyridine/acetic acid/water (65:2:5:3:29)] as described (Boyle et al., 1991). Phosphoamino acid analyses were carried out on phosphorylated proteins or on peptides recovered from two-dimensional maps as described (Kamps & Sefton, 1989; Cooper et al., 1983).

RESULTS

Phosphorylation of MAPKK by Mos

Recombinant MAPKK was phosphorylated with immunoprecipitates of v-Mos (Figure 1A) to stoichiometries ranging from 1.6 to 2.6 mol/mol after 15 h (Figure 1A). Phosphate incorporation correlated with MAPKK activation for up to 2 h (Mansour et al., 1994a). While the phosphate incorporation increased 2-fold further after 15 h (Figure 1A), no additional increase in MAPKK activation was seen (data not shown), a discrepancy most likely due to the instability of MAPKK after prolonged incubation. Phosphoamino acid analysis of v-Mos-phosphorylated MAPKK as well as autophosphorylated MAPKK revealed serine, tyrosine, and threonine phosphorylation (Figure 1B,C). Although the v-Mos immunoprecipitates contained weak Raf-1 immunoreactivity (<1% of the total Raf-1), Raf-1 immunoprecipitated from these extracts showed no significant phosphorylation of MAPKK, indicating that Raf-1 contamination could not account for the activity in Figure 1 (J. M. Candia and N. G. Ahn, unpublished observations). Further evidence that Mos directly phosphorylates MAPKK has been indicated by the interaction of Mos and MAPKK in a yeast two hybrid system (M. Chen and J. A. Cooper, personal communication).

Identification of Phosphopeptides in MAPKK

Tryptic/endoproteinase LysC digests of MAPKK were analyzed on capillary HPLC columns directly coupled to the mass spectrometer. MAPKK peptides were identified in LC/MS chromatograms by comparing observed masses to masses of predicted proteolytic fragments (Table 1). [For a depiction of the tryptic peptides within the MAPKK1 sequence, see Mansour et al. (1994b).] Combination of trypsin and endoproteinase LysC improved cleavage at K_{324} and produced partial cleavage at three internal KP sequences, but not at K_3, resulting in the incompletely proteolyzed fragment, Tp2/3 (Table 1). Peptide sequences were confirmed by MS/MS.

Phosphorylated peptides were identified as peptides with mass increases of 80 Da or multiples thereof. Significant levels of phosphorylation were observed at two sites on both Tp28 and Tp33 (Table 2). Minor levels of phosphorylation were observed at a third site on Tp33 and at two sites on Tp2/3 (Table 2). These sites accounted for 2.3 mol of phosphate/mol of MAPKK, accounting for most of the phosphate incorporation observed in parallel radiolabeling experiments (2.6 mol/mol in this experiment).

Although mass spectrometric ion intensities of peptides with different compositions cannot always be compared (because some peptides ionize more readily than others), relative yields of peptides that are nearly identical (for example, differing by one phosphate) can be obtained. This was confirmed by summing the ion intensities of the phosphorylated and nonphosphorylated forms of each peptide, after normalization to total ion currents of all MAPKK peptides (Mansour et al., 1994b). The summed intensities of the phosphorylated and nonphosphorylated peptides were comparable between v-Mos-phosphorylated wild-type MAPKK and unphosphorylated wild-type MAPKK, indicating that phosphorylation did not alter the recovery of peptides Tp2/3, Tp28, and Tp33.

Tp33 and Tp2/3 Are Intramolecular Autophosphorylation Sites

v-Mos-phosphorylated versus autophosphorylated sites were distinguished by comparing Tp2/3, Tp28, and Tp33 phosphorylation between wild-type and various mutants of MAPKK (Table 2). Upon incubation with v-Mos, a catalytically inactive mutant of MAPKK (referred to as K97M) was phosphorylated at two sites on Tp28. The levels of phosphorylation of this peptide were comparable to if not higher than those seen on wild-type MAPKK; moreover, autophosphorylated wild-type MAPKK had little phosphate on Tp28, indicating that two residues on this peptide were directly targeted by v-Mos. In contrast, phosphorylation of Tp2/3 and Tp33 was negligible in MAPKK (K97M), indicating that these peptides contain sites of autophosphorylation. This was confirmed by the efficient autophosphorylation of these peptides in a constitutively active mutant of MAPKK (ΔN3/S218E/S222D) (Mansour et al., 1994a). Wild-type MAPKK was more highly phosphorylated on Tp33 and Tp2/3 after v-Mos activation than after autophosphorylation, indicating that the activation of MAPKK enhances autophosphorylation at these sites.

Table 1: Masses of Peptides Observed in Digested Recombinant Human MAPKK and Rabbit Skeletal Muscle MAPKK

peptide number[a]	predicted mass (Da)[c]	recombinant MAPKK obs mass (Da)[e]	rabbit MAPKK obs mass (Da)[k]
Tp1	487.2[d]	487.3[f]	ns[l]
Tp2/3[b]	3277.5	3277.3	3277.8
Tp3	3149.5	3148.8	3149.4
Tp4/5	1529.7	1529.1	1529.4
Tp5	1401.5	1400.8	1400.8
Tp7/8	1104.6	1104.4	1105.2
Tp8	948.5	948.7	948.7
Tp10	544.3	544.2[f]	544.3
Tp10/11	1294.4	1293.9	1294.3
Tp11	767.3	ns[g]	767.4
Tp12	1347.5	1346.7	1347.1
Tp13	1281.6	1281.0	1281.4
Tp14/15	1430.8	1430.8	1430.3
Tp15	1302.6	1302.3[h]	1302.0
Tp16	642.4	ns	642.4
Tp17	4796.4	5006.2[i]	4794.7
Tp19/20	1180.7	1180.4	ns
Tp20	896.5	896.7	896.7
Tp21	728.5	728.5	728.8
Tp22	721.4	721.4	721.4
Tp25	555.3	ns	555.3
Tp26	1340.8	1341.0	1340.8
Tp27	445.3	ns	445.2
Tp28	2317.6	2422.6[j]	2393.4[m]
Tp29	868.4	868.3	868.7
Tp30	2865.3	2865.5	2865.0
Tp30/31	3844.4	ns	3843.4
Tp31	996.5	996.2	996.8
Tp32	2445.8	2550.6[j]	2522.1[m]
Tp33	3689.3	3688.4	3688.0
Tp33/34	5498.3	5497.8	5513.1[n]
Tp34	1827.1	1826.1	1841.0[n]
Tp35	475.3	580.6[j]	475.3
Tp35/36	1042.6	1147.8[j]	ns
Tp37	445.3	ns	445.2
Tp38	1085.6	1085.8	1086.0
Tp39/40	3230.5	3335.2[j]	3229.8
Tp40	3074.3	3179.2[j]	ns

[a] Tryptic peptides are numbered from the amino (Tp1) to carboxyl (Tp40) termini of human or rabbit MAPKK1 (Mansour et al., 1994b). Incomplete proteolytic products are indicated by two peptide numbers separated by a slash. Peptides that are absent from the LC/MS spectra of both proteins are not shown; these include seven single K or R residues, Tp2, Tp4, Tp6, Tp7, Tp14, Tp18, and Tp39; three dipeptides, Tp9, Tp23, and Tp24; and one tripeptide, Tp19. Peptides from the fusion domain amino-terminal to the first residue of MAPKK are shown shown; of the five possible peptides in this sequence, only WGSG-GVGSALPGSK was detected. [b] Two incomplete proteolytic products with this mass (Tp2/3 and Tp3/4) were predicted, containing an extra Lys at either the amino or carboxyl terminus, but only one (Tp2/3) was observed by LC/MS/MS. [Note that Tp2/3 contains residues 4−35 of MAPKK, and not residues 5−35, as was erroneously indicated in Figure 2 of Mansour et al. (1994b).] [c] Calculated from the amino acid sequence predicted from cDNA of human MAPKK1 (Seger et al., 1992b), using monoisotopic masses for peptides less than 1200 Da and average masses for peptides larger than 1200 Da. [d] Includes methionine at position 1. [e] Data are from LC/MS spectra (0.13 Da step size) of tryptic and tryptic/endopeptidase Lys C peptides from recombinant huamn MAPKK1 (alkylated with 4-vinylpyridine) eluting from C18 Vydac or C4 POROS 500 μm columns. [f] Only observed using the C18 Vydac column. [g] Not seen. [h] A peptide with mass 864.7 Da (predicted mass 864.6 Da), corresponding to cleavage of a KP sequence in this peptide, was also observed. [i] Includes 210 Da for the alkylation of two cysteine residues by 4-vinylpyridine. [j] Includes 105 Da for the alkylation of one cysteine residue by 4-vinylpyridine. [k] Data are from LC/MS spectra (0.25 Da step size) of tryptic peptides from rabbit skeletal muscle MAPKK1, eluting from an HP C18 250 μm column. [l] None of the possible variants were observed. [m] Includes 76.1 Da for the addition of 2-mercaptoethanol to one cysteine residue. [n] Human and rabbit MAPKK1 differ by one amino acid (G_{328} in human and A_{328} in rabbit) (Seger et al., 1992b; Ashworth et al. 1992). Predicted masses of rabbit Tp33 and Tp33/34 are 1841.1 and 5512.3 Da, respectively.

The mechanism of autophosphorylation was explored by incubating constitutively active MAPKK (ΔN3/S218E/S222D) with catalytically inactive MAPKK (K97M) in the presence of MgATP (Figure 2). Incorporation of radiolabel into constitutively active MAPKK but not catalytically inactive MAPKK was observed. The ability of MAPKK (ΔN3/S218E/S222D) to phosphorylate itself but not MAPKK (K97M) indicates that autophosphorylation of Tp33 and Tp2/3 occurs intramolecularly.

Identification of Phosphorylated Residues

Phosphopeptide Tp28 (Residues 206−227: LCDFGVS-GQLIDSMANSFVGTR). LC/MS/MS of non-, mono-, and diphosphorylated Tp28 (Figure 3A−D) yielded a series of sequence-specific y ions (y_1−y_{12}) encompassing the two phosphorylation sites. Phosphorylation was revealed by fragment ions with masses 80 Da greater (addition of phosphate) than those predicted for the unphosphorylated peptides. In addition, ions with masses 18 Da less than predicted were often observed, which resulted from the neutral loss of phosphoric acid (mass 98 Da) from serine or threonine, respectively, producing dehydroalanine or dehydrothreonine. The fragmentation of peptides containing dehydroalanine or dehydrothreonine is usually enhanced at the peptide bonds immediately adjacent to the dehydrated amino acid (K. A. Resing and R. S. Johnson, unpublished observations); however, this was not observed with Tp28, suggesting that neutral loss in this case occurred subsequent to peptide backbone cleavage.

The LC/MS chromatogram of monophosphorylated Tp28 (MH_3^{3+} = 835.2 Da/e) showed two ions separating with baseline resolution, eluting at 9.5 and 11.3 min (2%/min gradient). In the LC/MS/MS spectrum of the early eluting peptide (Figure 3C), fragment ions y_6−y_{12} were observed with mass shifts of +80 or −18 Da, revealing the presence of phosphate on S_{222}. Unphosphorylated y_6−y_{12} ions were completely absent from this spectrum, indicating that the early peptide was phosphorylated solely at this site. In contrast, partial fragmentation of the later eluting peptide revealed the presence of phosphate on S_{218}, with no evidence for S_{222} phosphorylation (Figure 3B). Thus, these two peptides, phosphorylated on different residues but otherwise identical, eluted from the reversed phase column with different retention times. This may reflect differing conformations adopted by the peptides, depending upon the site phosphorylated. Similar resolution by reversed phase HPLC of two monophosphorylated forms of Tp33a was also observed (see below).

Diphosphorylated Tp28 (MH_3^{3+} = 861.6 Da/e) produced fragment ions corresponding to y_6 + 80 through y_9 + 80 Da and y_{10} + 160 through y_{12} + 160 Da (Figure 3D). In addition, fragment ions corresponding to y_6 − 18 through y_8 − 18 Da and y_{10} − 36 through y_{12} − 36 Da were noted, reflecting the neutral loss of one and two phosphoric acid groups, respectively. Ions observed with masses y_{11} + 62 and y_{12} + 62 Da corresponded to diphosphorylated fragment ions that had lost one phosphoric acid group (62 Da = +160 − 98 Da). Taken together, the data on Tp28 demonstrate its phosphorylation at S_{218} and S_{222} within the sequence $LIDS_{218}MANS_{222}FV$.

In order to examine the kinetic order of phosphorylation, MAPKK was incubated for varying times with v-Mos, and Tp28 phosphorylation was analyzed by LC/MS and LC/MS/

Table 2: Stoichiometries of Tp2/3, Tp28, and Tp33 Phosphorylation for Wild-Type and Mutant MAPKK[a]

	wild-type MAPKK, +v-Mos (%)		MAPKK (K97M), +v-Mos (%)		wild-type MAPKK, autophosphorylated (%)		MAPKK(ΔN3/S218E/S222D), autophosphorylated (%)
peptide	expt 1	expt 2	expt 1	expt 2	expt 1	expt 2	expt 1
Tp28	24	13	28	24	100	100	100
Tp28+1P	61	68	36	21	0	0	0
Tp28+2P	15	19	36	55	0	0	0
Tp2/3	91	89	99	100	94	95	96
Tp2/3+1P	7	9	1.0	0	4	4	4
Tp2/3+2P	2	2	0	0	2	1	0
Tp33	32	31	97	97	89	90	41
Tp33+1P	38	39	3	3	11	10	31
Tp33+2P	27	29	0	0	0	0	24
Tp33+3P	3	0	0	0	0	0	4

[a] Ion intensities were quantified from LC/MS data for Tp2/3, Tp28, Tp33 and their multiply phosphorylated forms in wild-type MAPKK, catalytically inactive MAPKK(K97M), and constitutively active MAPKK(ΔN3/S318E/S222D). Stoichiometries are expressed as percent of total amount of peptide.

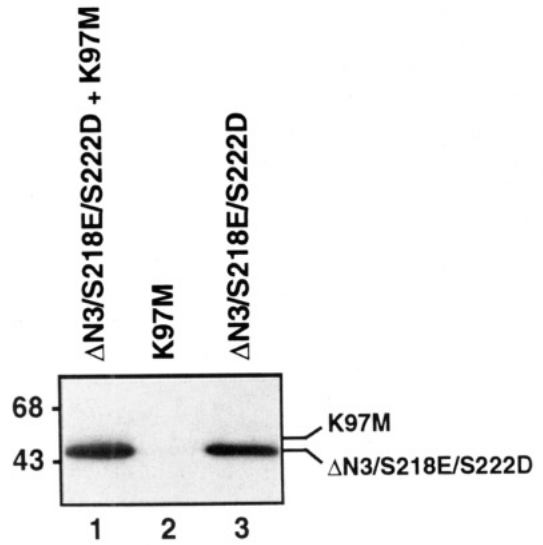

FIGURE 2: MAPKK autophosphorylation is intramolecular. Equal amounts (1.8 μg) of constitutively active MAPKK (ΔN3/S218E/S222D) and catalytically inactive MAPKK (K97M) were incubated in the presence of 10 mM $MgCl_2$/0.1 mM [γ-^{32}P]ATP (300 Ci/mol) for 3 h at 30 °C prior to separation by SDS−PAGE and autoradiography (lane 1). Controls containing MAPKK (K97M) (lane 2) or MAPKK (ΔN3/S218E/S222D) (lane 3) were performed in separate incubations. MAPKK (ΔN3/S218E/S222D), which contains a deletion of 20 amino acids, migrates faster than MAPKK (K97M) on SDS−PAGE as indicated.

MS. Levels of Tp28 monophosphorylated at S_{222} increased with the time of incubation. In comparison, Tp28 monophosphorylated at S_{218} was predominant at $t = 0$, but remained essentially unchanged from 0.5 to 15 h (Figure 4A). Diphosphorylated Tp28 increased with time (although the levels of this peptide were low in this experiment). The data indicate that the rate of S_{222} phosphorylation by v-Mos is faster than that of S_{218}, implying kinetically ordered phosphorylation during the activation reaction. In addition, S_{218} represents a weak autophosphorylation site on Tp28 (also see Table 2).

Phosphorylation of S_{218} and S_{222} by v-Mos was then compared between several MAPKK mutants containing alanine in place of each of four phosphorylatable residues in Tp28 (S_{212}, S_{218}, S_{222}, and T_{226}). Levels of Tp28 monophosphorylated on S_{218} in the S222A mutant or on S_{222} in the S218A mutant were comparable to that of wild-type MAPKK (Figure 4B), indicating that the accumulation of monophosphorylated Tp28 in the time course (Figure 4A) reflects the relative rates of phosphorylation at these two sites; furthermore, phosphorylation at one site is not required for the other. Significantly, when either S_{218} or S_{222} was mutated to alanine, the activation of MAPKK by v-Mos was reduced compared to that of wild-type MAPKK, but was not completely suppressed (Figure 4C), indicating that phosphorylation at either site was sufficient to partially activate MAPKK.

Phosphopeptide Tp33 (Residues 292−324: TPGRPLSSYG-MDSRPPMAIFELLDYIVNEPPK). LC/MS/MS of the non- and monophosphorylated Tp33 peptides resulted in efficient fragmentation through the COOH-terminal half of each peptide (residues 309−324), with no evidence for phosphorylation within this region (data not shown). In order to sequence the NH_2-terminal half of this peptide, tryptic/endoproteinase LysC digests were proteolyzed further with endoproteinase AspN, cleaving Tp33 into Tp33a (residues 292−302), Tp33b (residues 303−314), and Tp33c (residues 315−324). Non-, mono-, and diphosphorylated Tp33a peptides were apparent in the LC/MS chromatogram, but no phosphate was found on Tp33b or Tp33c (confirmed by LC/MS/MS, data not shown). These findings, combined with the absence of phosphate from residues 309−324 of Tp33, indicate that the major phosphorylation sites occur within Tp33a.

Tp33a (Residues 292−302: TPGRPLSSYGM). LC/MS/MS of nonphosphorylated Tp33a (MH_2^{2+} = 583.6 Da/e) led to the cleavage of all peptide bonds except those between GR and PL (Figure 5A). A complex fragmentation pattern was observed, with many secondary cleavages that yielded internal fragment ions, losses of H_2O and NH_3, and iminium ions, including an intense iminium ion of tyrosine at 135.9 Da/e (not shown). Several MAPKK mutants with amino acid substitutions at phosphorylation sites were analyzed to facilitate the identification of product ions in the Tp33a MS/MS spectrum (Figure 5).

LC/MS/MS of monophosphorylated Tp33a (MH^{2+} = 623.4 Da/e) revealed two peaks of identical mass eluting at 18.7 and 22.1 min, corresponding to isoforms that resolved by HPLC (1%/min gradient). The MS/MS spectrum of the early (18.7 min) peak (Figure 5B) showed mass shifts of +80 Da for b_9 and b_{10} ions, but not for b_8, indicating phosphorylation at Y_{300}. In agreement, a y_3 + 80 Da ion and the 215.9 Da/e iminium ion of phosphotyrosine (but not of tyrosine) were present (data not shown). Ions resulting from the neutral loss of H_3PO_4 were absent from this

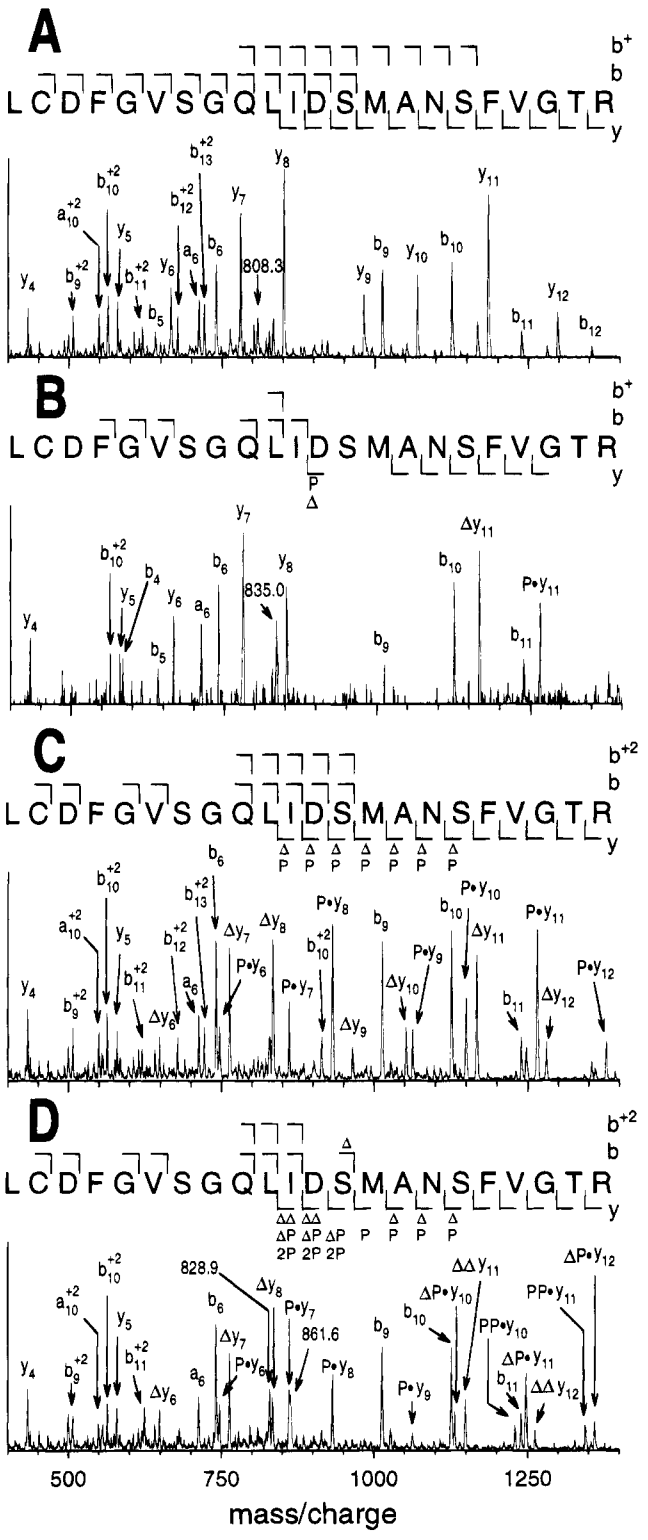

FIGURE 3: MS/MS of (A) Tp28 (MH_3^{3+} = 808.3 Da/e), (B) Tp28 + 80 Da (one phosphate) early eluting peak (MH_3^{3+} = 835.0 Da/e), (C) Tp28 + 80 Da late eluting peak, and (D) Tp28 + 160 Da (two phosphates) (MH_3^{3+} = 861.6 Da/e). Scans across the entire LC range were surveyed for each mass in order to detect isomeric forms. The monophosphorylated isoform in panel B was present at a very low level, producing a spectrum of poor quality. Each spectrum represents the summation of several scans that were acquired as each component of the tryptic/endoproteinase Lys C digest eluted from the HPLC column. The mass spectrometer was scanned from 100 to 1600 Da/e; for clarity, each panel shows only the region between y_4 and y_{12}, which is most relevant to the location of phosphate. The *m/z* of the precursor (or parent) ion is labeled in each case, except in (C) where no precursor ion remained after collisional activation; in (D) an ion with the mass of the H_3PO_4 neutral loss product of the parent ion is labeled (828.9 Da/e). Fragmentation produced a series of ions with sequence-dependent increments in mass. For example, y_4 = 432.3 Da/e and y_5 = 579.3 Da/e, respectively, represent the fragment ions VGTR and FVGTR, increasing by the mass of phenylalanine (147 Da). A series of singly charged y ions from y_1 through y_{12} were observed, along with overlapping sets of singly and doubly charged b ions encompassing b_2–b_{17}. Symbols indicate ions shifted in *m/z* from that predicted by the amino acid sequence by +80, +160, −18, −36, or +62 Da, respectively, representing the addition of one or two phosphates (P• or PP•), the neutral loss of one or two H_3PO_4 groups (Δ or ΔΔ), or the addition of one phosphate plus the neutral loss of one H_3PO_4 (ΔP•). The same changes in the doubly charged fragment ions create *m/z* shifts of +40, +80, −9, −18, or +31 Da. Each panel also shows the peptide sequence with a summary of the observed ions, where singly and doubly charged b ions (b and b^{2+}) are displayed above the sequence (⌉), and singly charged y ions (y) are shown below (⌊). A Δ or P in the summary indicates that the ion corresponding to the mass of the derivative ion was observed, *with no detectable underivatized ion*. For clarity, lower intensity ions are not labeled, including internal fragment ions, a type ions, and ions with the loss of ammonia or water.

spectrum, as would be expected from the known resistance of phosphotyrosine to this type of fragmentation.

The total intensity of the late (22.1 min) peak was 3.5 times lower than that of the early peak, indicating lower abundance of the second isoform. LC/MS/MS (Figure 5C) revealed the presence of ions corresponding to b_7 − 18 through b_{10} − 18 Da, whereas unaltered b_2 and b_4 ions were observed. Likewise, y_7 − 18, y_9 − 18, and y_{10} - 18 Da were found, but y_1−y_4 were intact. By comparison with the unphosphorylated peptide (Figure 5A), this fragmentation pattern is most consistent with the phosphorylation of S_{298}. A disproportionately high yield of y_4 suggested that, unlike Tp28, neutral loss of H_3PO_4 from Tp33a preceded cleavage at this bond.

Diphosphorylated Tp33a (MH_2^{2+} = 663.4 Da/e) eluted as a single peak on HPLC. Both the neutral loss of H_3PO_4 from the parent ion (producing an ion of 614.4 Da/e, Figure 5D) and the generation of the phosphotyrosine iminium ion (215.9 Da/e, data not shown) were apparent in the LC/MS/MS spectrum, suggesting that both S_{298} and Y_{300} were phosphorylated in this peptide. These phosphorylation sites were best established by cleavages between SS and SY, producing b_7 − 18 and b_8 − 18 Da ions, which indicated phosphorylation at S_{298}. Curiously, b ions of higher mass were reduced in abundance; however, increases in the corresponding doubly charged b ions were observed, providing critical information for sequence determination. Predicted ion masses, assuming dehydroalanine in place of S_{298} and phosphotyrosine at Y_{300}, accounted for 98% of the ion intensity. No evidence for phosphorylation at T_{292} was apparent in any of the analyses of recombinant MAPKK (including possible incomplete proteolytic products that might have resulted from the inhibition of cleavage).

In order to corroborate the LC/MS/MS results, several MAPKK mutants were constructed in which the major phosphorylation sites in Tp33, S_{298} and Y_{300}, were converted to alanine and phenylalanine, respectively (Figure 6). Unexpectedly, phosphorylation of an MAPKK(S298A) mutant still yielded non-, mono-, and diphosphorylated forms of Tp33a in LC/MS chromatograms. LC/MS/MS of the monophosphorylated T33a ion (MH_2^{2+} = 615.5 Da/e) derived from this mutant showed two peaks, eluting at 18.9 (13% of total) and 20.9 min (87% of total). The MS/MS spectrum of the first (18.9 min) peak established the phosphorylation of Y_{300}.

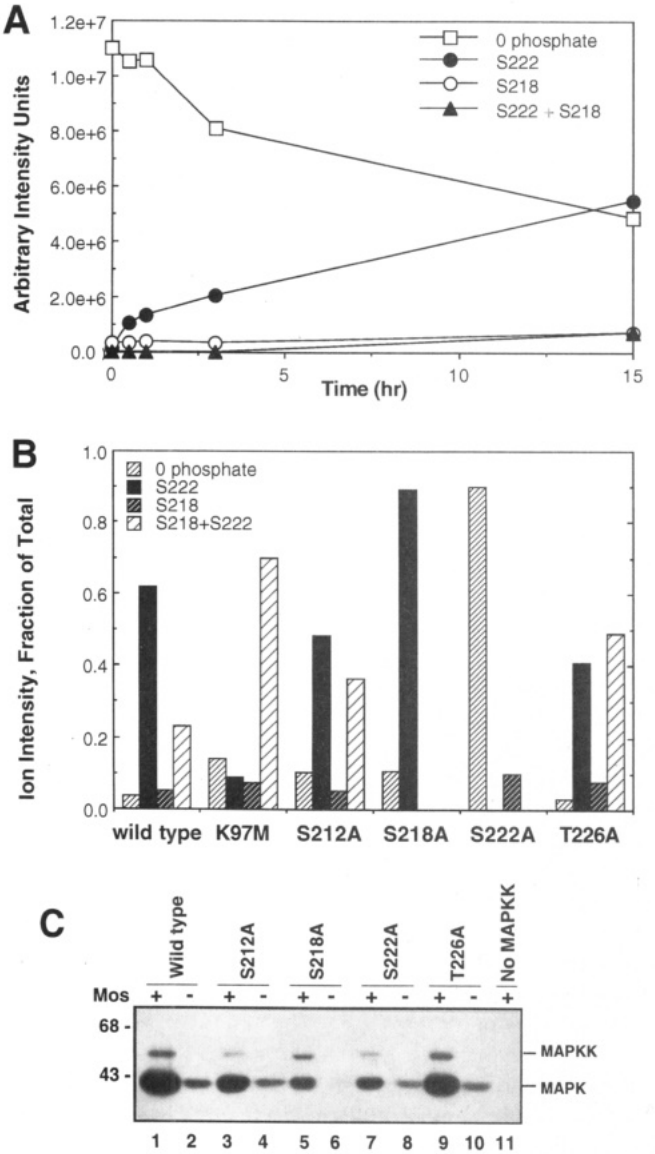

FIGURE 4: v-Mos-catalyzed phosphorylation sites on recombinant MAPKK; analysis of Tp28 phosphorylation at S_{218} and S_{222}. (A) MAPKK was phosphorylated for varying times by v-Mos as described in Materials and Methods, and relative amounts of non-, mono-, and diphosphorylated Tp28 were quantified from LC/MS spectra. Monophosphorylated Tp28 was further analyzed by LC/MS/MS as in Figure 3B,C in order to distinguish phosphorylation on S_{218} from that on S_{222}. The *y* axis is ion counts per second. (B) MAPKK mutants containing amino acid substitutions at the indicated residues were phosphorylated for 15 h with v-Mos, and relative amounts of each phosphorylated form of Tp28 were quantified as in (A). The difference between the wild type in this panel and the 15 h time point in panel A is most likely due to variations in the v-Mos activity in different experiments. (C) MAPKK mutants were phosphorylated in the presence (lanes 1, 3, 5, 7, and 9) or absence (lanes 2, 4, 6, and 8) of v-Mos for 15 min, prior to the addition of catalytically inactive ERK2 (K52R), as described in Materials and Methods. SDS−PAGE migration of MAPKK and MAPK(ERK2) are indicated on the right.

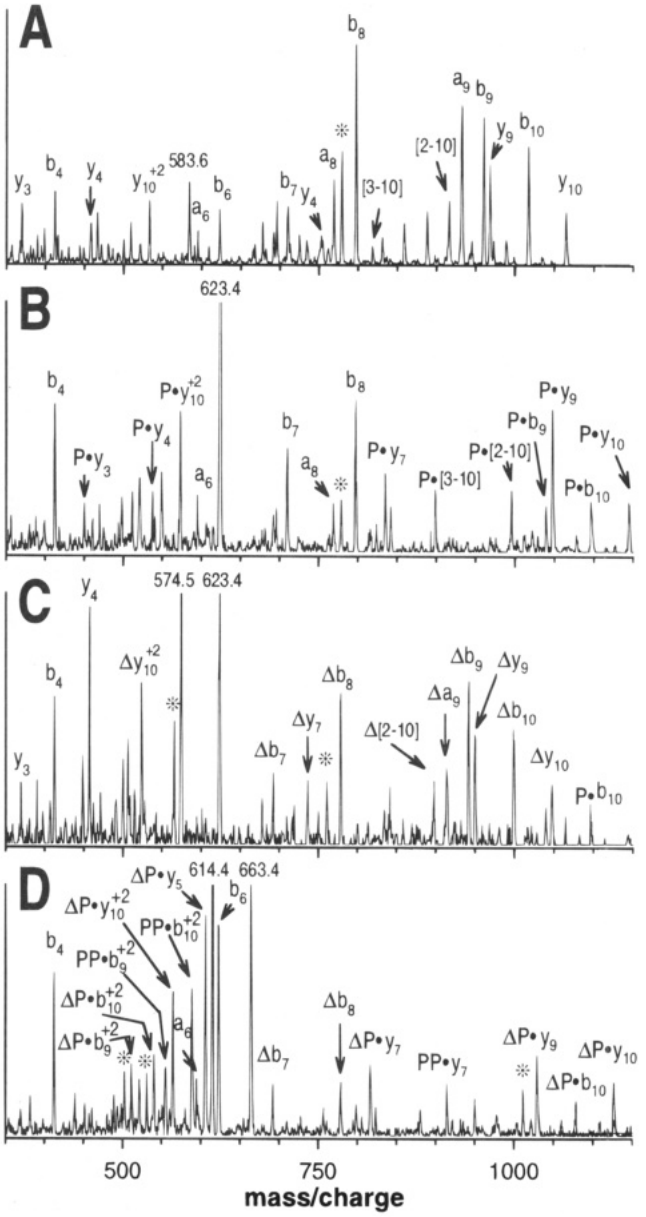

FIGURE 5: Identification of the major autophosphorylation sites in recombinant MAPKK. MS/MS of (A) Tp33a (MH_2^{2+} = 583.6 Da/e), (B) Tp33a + 80 Da (one phosphate) early eluting peak (MH_2^{2+} = 623.4 Da/e), (C) Tp33a + 80 Da late eluting peak, and (D) Tp33a + 160 Da (two phosphates) (MH_2^{2+} = 663.4 Da/e). The mass spectrometer was scanned from 100 to 1800 Da; however, each panel shows only the region of the spectrum relevant to the location of phosphate. Ions are labeled as described for Figure 3. Summaries of the observed ions in these peptides (including ions not shown in these spectra) are included in Figure 6. The *m/z* of the precursor ion is shown in each spectrum; in (C) and (D), ions of 574.5 and 614.4 Da/e, respectively, indicate the neutral loss of H_3PO_4 from the parent ions. The b_6 ion of (B) has the same predicted mass as the precursor ion; its presence is suggested by the observation of the a_6 ion. a_6 and b_6 were not observed in (C). Bracketed numerals indicate internal fragment b ions (e.g., [2−10] corresponds to an internal fragment between residues 2 and 10 of the peptide). Asterisks indicate the loss of H_2O (−18) from a higher mass ion.

The MS/MS spectrum of the second (20.9 min) peak exhibited a neutral loss of H_3PO_4; the appearance of b_7 together with $b_8 - 18$ through $b_{10} - 18$ Da ions demonstrated phosphorylation at S_{299} (summarized in Figure 6). Only non- and monophosphorylated forms of Tp33a were observed in MAPKK containing the mutation of Y_{300} to phenylalanine. The LC/MS/MS spectrum of the monophosphorylated Tp33a ion (MH_2^{2+} = 615.5 Da/e) contained $b_7 - 18$ through $b_{10} - 18$ ions, indicating phosphorylation at S_{298}. Mutagenesis of S_{299} to valine yielded peptides phosphorylated on S_{298} and Y_{300}, indistinguishable from the behavior of wild-type MAPKK (Figure 6).

MAPKK mutants containing substitutions at each of the phosphorylatable residues in Tp33a (S298A, S299V, and Y300F) were tested for activation in vitro by v-Mos. No differences were observed in the amount of basal or v-Mos-

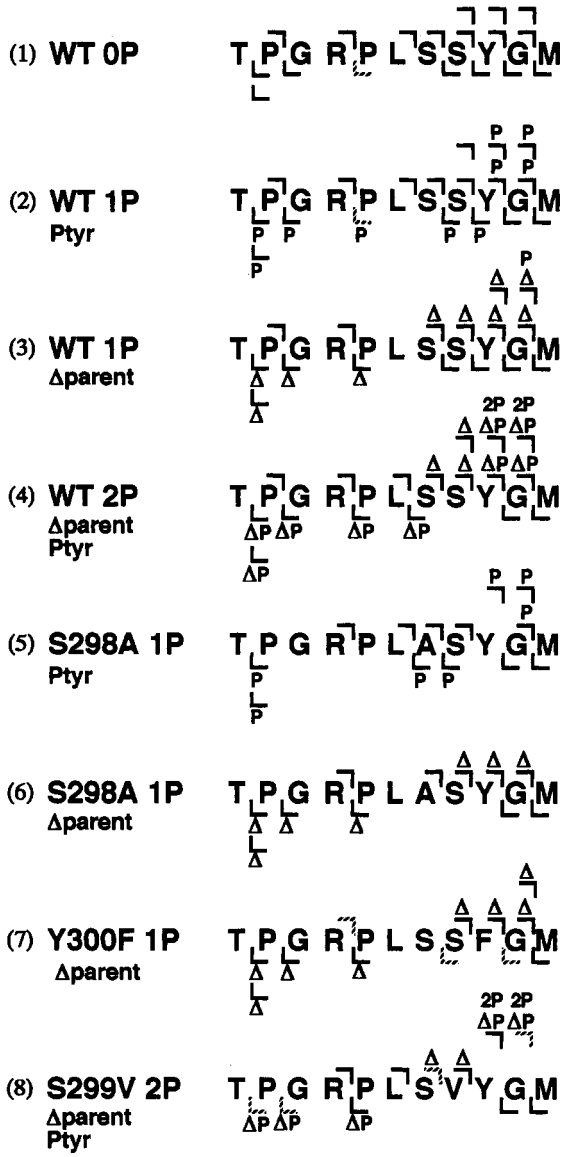

FIGURE 6: Summary of MS/MS spectra for Tp33a derived from wild-type and Tp33 mutants. Rows 1−4: Observed fragment ions in non-, mono-, and diphosphorylated Tp33a from wild-type MAPKK are indicated, corresponding to the spectra shown in Figure 5A−D, respectively. Rows 5 and 6: Summary of fragment ions from the two monophosphorylated forms of MAPKK(S298A) (MH_2^{2+} = 615.3 Da/e). Row 7: Summary of fragment ions from the monophosphorylated MAPKK(Y300F) (MH_2^{2+} = 615.3 Da). Row 8: Summary of fragment ions from the monophosphorylated MAPKK(S299V) (MH_2^{2+} = 629.3 Da). Observed fragment ions are indicated with singly and doubly charged b ions shown above the sequence (⌈) and singly charged y ions shown below the sequence (⌊); dotted ⌉ and ⌋ indicate ions with intensity less than 5 times background. Symbols indicate the presence of fragment ions with predicted *m/z* corresponding to the neutral loss of H_3PO_4 (Δ) and/or phosphorylation (P•), along with the absence of their unmodified forms. Spectra of the two forms of singly phosphorylated peptide derived from the wild-type spectra (rows 2 and 3) had a weak b_2 along with an intense a_2. The b_6 ions of these two peptides have the same *m/z* as the parent ion; an a_6 ion was present only in the phosphotyrosine form (row 3). In S299V (row 8), only the doubly phosphorylated form is shown; two singly phosphorylated forms were observed, with spectra similar to those seen in the singly phosphorylated forms of the wild-type Tp33a. Ptyr indicates the presence of the iminium ion of phosphotyrosine; Δparent indicates the presence of an ion of *m/z* corresponding to the neutral loss of H_3PO_4 from the parent ion.

stimulated phosphate incorporation into ERK2(K52R) compared to wild-type MAPKK (data not shown).

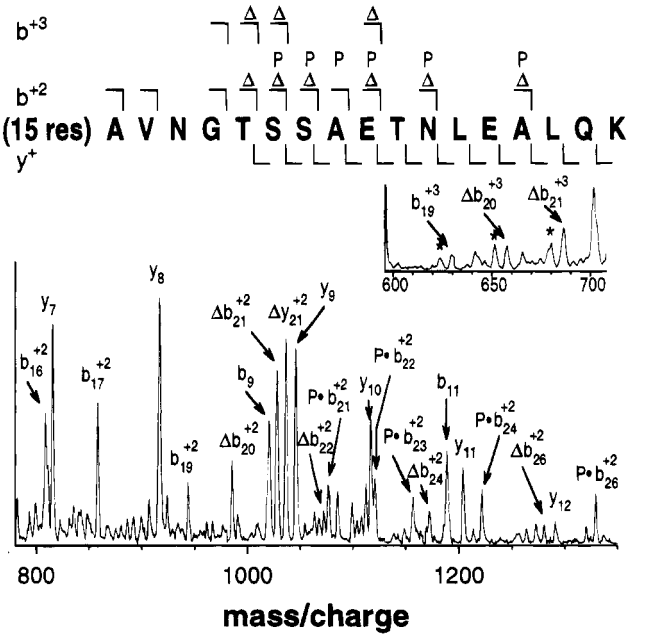

FIGURE 7: Identification of a minor autophosphorylation site in Tp2/3 from recombinant MAPKK. MS/MS of Tp2/3 + 80 Da (MH_3^{3+} = 1120.2 Da), showing the region of spectrum relevant to the location of phosphate on T_{23}. Ions are labeled as described for Figure 3. The region of the spectrun containing the ions corresponding to b_{19}^{3+}, Δb_{20}^{3+}, and Δb_{21}^{3+} is shown in the inset. Asterisks indicate the loss of water (resulting in an additional loss of 18 Da from Δb_{20}^{3+} and Δb_{21}^{3+}). A summary of the ions observed in the MS/MS spectrum is shown, with b^{2+} and b^{3+} ions displayed above the sequence (⌈) and y^+ ions shown below (⌊); the sequence shown begins with residue 16. The complete spectrum also shows b_1, b_2, b_6-b_9, b_{11}, b_{23}, b_9^{2+}, b_{15}^{2+} − 18, and y_1-y_6 ions. The identification of y_{21}^{2+} + 40 (1085.4 Da/e) was supported by the presence of a 1045.0 Da/e ion in the unphosphorylated Tp2/3.

Phosphopeptide Tp2/3 (Residues 4−35: KKPTPIQLNPAPDGSAVNGTSSAETNLEALQK). The LC/MS/MS spectrum of monophosphorylated Tp2/3 (MH_4^{4+} = 840.4 Da/e) showed one site of phosphorylation at T_{23} (Figure 7). The presence of two adjacent serines complicated the analysis because of the tendency of these three residues to lose H_2O, even when not phosphorylated. The assignment of phosphate to T_{23} was implied by the absence of phosphorylation on y_1-y_{12} and by the presence of several b^+ and b^{2+} ions as large as b_{19}. The assignment was further supported by the presence of phosphorylated b_{21}^{2+} + 40 through b_{24}^{2+} + 40 Da/e ions and by the corresponding b_{20}^{2+} − 9 through b_{24}^{2+} − 9 Da/e ions, suggesting the neutral loss of H_3PO_4 from fragment ions containing T_{23}, with complete loss from the b_{20}^{2+} ion. There were also triply charged b ions with *m/z* corresponding to the cleavage within the GTSS sequence (insert), which could be interpreted as the complete loss of neutral loss of H_3PO_4 from T_{23} in these ions. Autophosphorylation of T_{23} was confirmed by substituting this residue with alanine. Two-dimensional phosphopeptide mapping of this mutant, autophosphorylated in absence of v-Mos, showed the loss of a phosphothreonine-containing peptide that was present in maps of wild-type MAPKK (data not shown).[2]

LC/MS/MS spectra of diphosphorylated Tp2/3 derived from wild-type MAPKK phosphorylated by v-Mos were

[2] These two-dimensional maps of autophosphorylated MAPKK also identified a third peptide phosphorylated on tyrosine, as determined by phosphoamino acid analysis. Mutational analysis showed that the phosphotyrosine was in a peptide not found by LC/MS, which was amino-terminal to the first methionine of MAPKK, within the sequence DLYDDDDK.

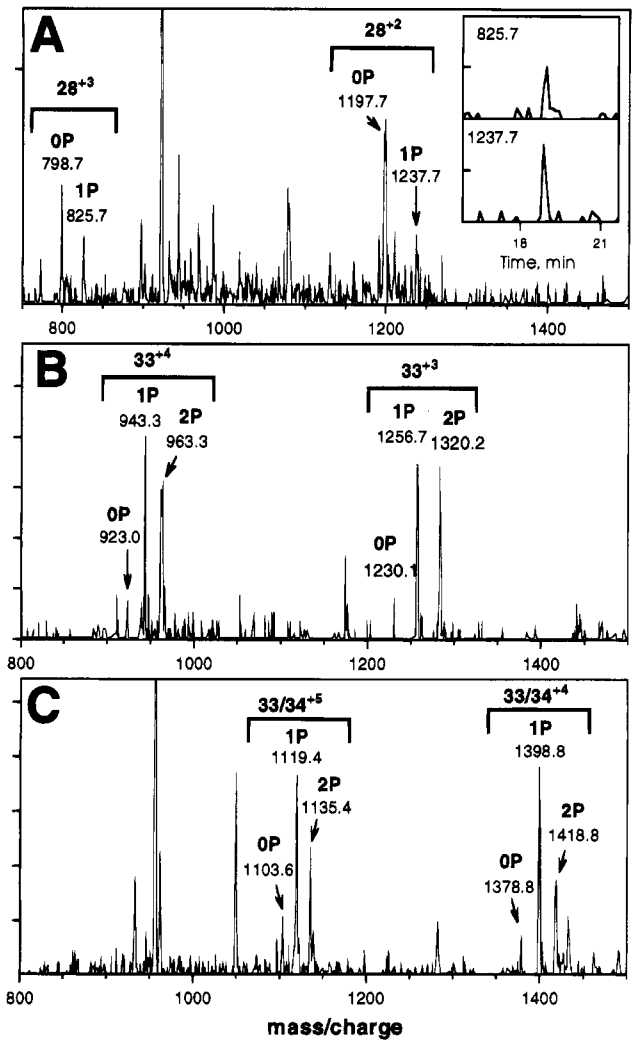

FIGURE 8: LC/MS spectra of (A) Tp28, (B) Tp33, and (C) Tp33/34 from purified rabbit skeletal muscle MAPKK. A tryptic digest of MAPKK was analyzed by LC/MS, as described in Materials and Methods. To obtain the spectra shown, several scans that encompassed the peptides of interest were summed. This procedure tends to increase the background noise, which is particularly high in panel A. To demonstrate the signal to noise ratio for the monophosphorylated Tp28, signals from the individual *m/z* ions of this peptide are plotted against HPLC elution time (inset in panel A). Only the relevant ions are labeled in each spectrum; the other ions present are from other peptides of MAPKK (including 1198.9 Da/e, eluting close to nonphosphorylated $Tp28^{2+}$ and 962.1 Da/e eluting close to diphosphorylated $Tp33^{4+}$).

uninformative due to the low signal intensity of the parent ion (data not shown). However, the LC/MS/MS spectrum of monophosphorylated Tp2/3 derived from MAPKK(T23A) revealed a second site of phosphorylation, most likely occurring at S_{24}, although phosphorylation at S_{25} could not be ruled out. MAPKK mutants containing substitutions at each of the phosphorylatable residues of this peptide (T23A, S24A, and S25A) were tested for activation in vitro by v-Mos. No differences were observed in basal or v-Mos-stimulated activity compared to wild-type MAPKK (data not shown).

Physiological Phosphorylation of Tp28 and Tp33

Highly purified active skeletal muscle MAPKK (2 pmol) was digested with trypsin and analyzed by LC/MS in order to examine in vivo sites of phosphorylation (Figure 8). The identified MAPKK peptides accounted for 92% of the ion intensity observed and included all of the phosphorylatable peptides in rabbit MAPKK1 (Ashworth et al., 1992). Tp28 and Tp32, each containing one cysteine residue, were observed with mass shifts of +76 Da, indicating adduct formation with β-mercaptoethanol. Non- and monophosphorylated Tp28's were observed in a ratio of 3:2, but a diphosphorylated Tp28 was not observed (Figure 8A). Tp2/3 was recovered in good yield but was not phosphorylated, suggesting that autophosphorylation at this site may be insignificant in vivo. Ions with masses corresponding to mono- and diphosphorylated Tp33 and Tp33/34 were observed in approximately equal yields, along with lower amounts of nonphosphorylated peptides (Figure 8B,C). Triphosphorylated Tp33/34 ions were also detected at very low levels. Phosphate was absent from Tp34, indicating that the phosphate on Tp33/34 was localized to Tp33. The HPLC retention times and charge distribution of these ions were similar to those observed with Tp33 and Tp33/34 in recombinant human MAPKK. Tp40, which contains T_{386}, a known site of phosphorylation by MAPK, was not observed as a phosphopeptide.

DISCUSSION

In this study, electrospray ionization mass spectrometry was used to examine the phosphorylation and activation of MAPKK by v-Mos as a model for c-Mos-mediated oocyte maturation, which involves the activation of MAPKK and MAPK (Matsuda et al., 1992; Posada et al., 1993; Nebreda & Hunt, 1993). Two phosphorylation sites were found to be targeted by v-Mos, and five residues were identified as autophosphorylation sites. In addition to providing information about the mechanism of MAPKK activation by Mos, mass spectrometry facilitated the discrimination between differentially phosphorylated forms of each phosphopeptide, which would have been difficult to distinguish by traditional methods of phosphorylation site analysis.

LC/MS/MS provided evidence for direct phosphorylation of S_{218} and S_{222} by v-Mos. In addition, S_{218} was observed to be an autophosphorylation site. These sites are identical to those previously shown to be targeted by Raf-1 (Alessi et al., 1994). Other investigators have utilized site-directed mutagenesis to indirectly implicate the same sites in the regulation of MAPKK by Raf-1, STE11, MEK kinase, and several MAPKK kinase activities from *Xenopus laevis* (Zheng & Guan, 1994; Alessi et al., 1994; Neiman & Herskowitz, 1994; Yan & Templeton, 1994; Gotoh et al., 1994, Huang & Erikson, 1994). Together the data suggest that MAPKK is activated in vitro by upstream kinases that phosphorylate the same residues. The ability of MAPKK to autophosphorylate on S_{218} indicates that autoactivation involves phosphorylation at sites targeted by exogenous kinases.

S_{298} and Y_{300} in the Tp33 sequence, $GRPLS_{298}SY_{300}GMD$, and T_{23} in the Tp2/3 sequence, $AVNGT_{23}SSAET$, were identified as autophosphorylation sites in this study. Both sites contain clustered phosphorylatable residues similar to a motif found in the sequence FLpTEpYVAT in ERK1 and ERK2, which are the only known exogenous substrates for MAPKK. Because synthetic peptides based on the ERK1/ERK2, Tp2/3, or Tp33 sequences were not substrates for MAPKK (A. S. Hermann, S. J. Mansour, and N. G. Ahn, unpublished results), tertiary structural determinants are likely to be important for defining MAPKK specificity. Neverthe-

less, the sequence similarities between the intramolecular and intermolecular phosphorylation sites may reflect specificity determinants for MAPKK. Interestingly, mutations at two of the autophosphorylated sites produced compensating increases in autophosphorylation at neighboring residues. This, together with the fact that at least two peptides are intramolecularly accessible to the active site in vitro, suggests some flexibility in the interaction of these sequences with the catalytic site.

MAPKK(S298A), MAPKK(S299V) or MAPKK(Y300F) mutants were comparable to wild-type MAPKK in their stimulation by v-Mos in vitro, indicating that autophosphorylation is not required for MAPKK activation. However, the Mos-catalyzed phosphorylation of Tp28 in wild-type MAPKK was somewhat reduced compared to that in catalytically inactive MAPKK (Table 2 and Figure 4B), suggesting that autophosphorylation might partially retard the second site phosphorylation by Mos or that v-Mos may be subject to feedback inhibition by MAPKK.

LC/MS analysis of MAPKK purified from skeletal muscle allowed us to assess the phosphorylation state of the enzyme in vivo. Phosphorylated Tp2/3 peptides were not observed in muscle MAPKK; thus, autophosphorylation at these sites may not occur physiologically. In contrast, intense ions corresponding to Tp33+80 and Tp33+160 and weak ions corresponding to Tp33+240 were observed, demonstrating significant phosphorylation of Tp33 under physiological conditions.

In addition to the two major and one minor autophosphorylation sites, Tp33 contains residue T_{292}, one of two sites recognized by MAPK (Saito et al., 1994; Gardner et al., 1994; Brunet et al., 1994; Mansour et al., 1994b). Phosphorylation of T_{292} has been demonstrated in tryptic phosphopeptide mapping studies of ^{32}P-labeled MAPKK from intact cells (Saito et al., 1994; Brunet et al., 1994), suggesting that this residue may represent one of the phosphorylated sites in Tp33 from the purified muscle enzyme. In vitro, no effect of MAPK phosphorylation on MAPKK activation has been observed (Saito et al., 1994; Mansour et al., 1994b); however, in intact cells, MAPKK activity appears to be enhanced by the mutation of T_{292} and T_{386} to alanine (Brunet et al., 1994). Presumably, the other phosphorylated residues observed on Tp33 from muscle MAPKK are represented by autophosphorylation sites. The MAPK-catalyzed and autophosphorylation sites in Tp33 are clustered near proline-rich amino acid sequences located between subdomains X and XI of the consensus kinase catalytic sequence. Sequence alignment of MAPKK with ERK2 and inspection of the X-ray structure of ERK2 (Zhang et al., 1994) would predict an insertion of Tp33 before the α_G-helix in the lower lobe of the kinase. Such a loop could plausibly have access to the kinase catalytic site. We speculate that although the phosphorylation sites on Tp33 may not necessarily be required for MAPKK activation by upstream kinases, phosphorylation of these residues might modulate potential interactions of MAPKK with substrates or other proteins that interact with the catalytic site. Furthermore, the high level of phosphorylation of Tp33 compared to Tp28 in vivo indicates that dephosphorylation of these sites may occur at different rates.

Our analysis of the phosphorylation and activation of MAPKK by Mos revealed several similarities to the phosphorylation and activation of MAPK by MAPKK. Like MAPKK, MAPK is activated upon phosphorylation at two sites residing in the T loop of subdomain VIII in the consensus catalytic sequence [as defined by Hanks and Quinn (1991)]. At least one residue in each case is a weak autophosphorylation site, represented by Y_{185} in ERK2(Robbins et al., 1993; Rossomando et al., 1992) and S_{218} in MAPKK. In both cases, phosphorylation at the two sites is kinetically ordered. Phosphorylation of Y_{185} is reported to be favored over T_{183} in ERK2 (Robbins & Cobb, 1992; Haystead et al., 1992), and phosphorylation of S_{222} is favored over S_{218} in MAPKK. However, in neither case is the order of catalysis obligatory, since finite phosphorylation of the alternate site is still observed in wild-type or mutant MAPK or MAPKK (Her et al., 1993; Robbins et al., 1993; Posada & Cooper, 1992).

In contrast, whereas the activation of ERK2 requires the phosphorylation of both T_{183} and Y_{185}, our data indicate that phosphorylation of either S_{218} or S_{222} is sufficient to activate MAPKK. This was demonstrated through partial activation by v-Mos of MAPKK mutants containing individual substitutions at each site (Figure 4C). Furthermore, LC/MS data in this study showed stoichiometries of Tp33 phosphorylation that were consistently higher than those of the doubly phosphorylated Tp28 peptide (Table 2). Because autophosphorylation is intramolecular (Figure 2), these data indicate that MAPKK does not have to be phosphorylated at a second site in order to catalyze Tp33 autophosphorylation. Significantly, diphosphorylated Tp28 was absent from purified skeletal muscle MAPKK. In this light, it is noteworthy that S_{218} phosphorylation is not required for in vitro activation by STE11, a homolog of MEKK (Gotoh et al., 1994), determined in studies employing MAPKK mutants in S_{218} and S_{222}. Similar conclusions were suggested by Alessi et al. (1994), who found that dephosphorylation of a threonine residue at position 218 was insufficient to inactivate MAPKK.

The present study employed a high-pressure collision cell, which resulted in surprisingly efficient cleavage of large peptides in the 2400−3300 Da range. These data provide insights into the effects of phosphorylation on peptide fragmentation in the gas phase, a subject that, with a few exceptions [for example, see Gibson and Cohen (1990); Palczewski et al., 1992] has largely been unexplored. With an earlier collision cell design, the neutral loss of H_3PO_4 from phosphopeptides was commonly observed in MS/MS, accompanied by a substantial reduction in peptide backbone cleavage, presumably due to the dissipation of vibrational energy upon neutral loss. Although the actual order of the fragmentation steps is uncertain, in the high-pressure collision cell, the initial cleavage of the large phosphopeptides (Tp28, Tp33, and Tp2/3) apparently occurred at the peptide backbone, followed by variable loss of H_3PO_4 from the fragment ions. In these studies, phosphorylation often led to changes in the ion chemistry. For example, the small peptide Tp33a showed decreased internal fragmentation and reduced b type ion yields that were more pronounced with increasing phosphorylation. This could not be due to the neutral loss of H_3PO_4, as similar changes occurred with tyrosine phosphate. Despite the influence of phosphorylation on peptide cleavage, sufficient fragmentation occurred at critical sites to allow unambiguous interpretation of the spectra.

The increased information content of mass spectral data compared to traditional methods of analysis gives the protein chemist a powerful tool for protein phosphorylation research. In this paper, we have demonstrated the feasibility of using

mass spectrometry to explore the complex phosphorylation of MAPKK without peptide purification and its attendant losses. Simultaneous determination of the stoichiometries of phosphorylation on all sites yielded further insight into the dependence of MAPKK activity on phosphorylation and autophosphorylation.

ACKNOWLEDGMENT

We thank Dr. Ken Walsh and Lowell Erickson for helpful discussions and for providing mass spectrometer facilities for initial studies, Dr. Martin McDermott and John Hunt, Synergen Inc., for providing access to the API-III, Greg Aiollo, Perkin Elmer, for advice on mass spectrometry, Mark Kissinger for technical assistance with cell culture, Dr. Wayne Matten for antibodies to v-Mos, and Dr. Jon Cooper for critical reading of the manuscript.

REFERENCES

Alessi, D. R., Saito, Y., Campbell, D. G., Cohen, P., Sithanandam, G., Rapp, U., Ashworth, A., Marshall, C. J., & Cowley, S. (1994) *EMBO J. 13,* 1610−1619.

Ashworth, A., Nakielny, S., Cohen, P., & Marshall, C. (1992) *Oncogene 7,* 2555−2556.

Biemann, K. (1990) *Methods Enzymol. 193,* 886−887.

Boyle, W. J., Van der Geer, P., & Hunter, T. (1991) *Methods Enzymol. 201,* 110−149.

Brunet, A., Pages, G., & Pouyssegur, J. (1994) *FEBS Lett. 346,* 299−303.

Cooks, R. G. (1978) *Collision Spectroscopy,* Plenum, New York.

Cooper, J. A., Sefton, B. M., & Hunter, T. (1983) *Methods Enzymol. 99,* 387−402.

Davis, M. T., & Lee, T. D. (1992) *Protein Sci. 1,* 935−944.

Dent, P., Haser, W., Haystead, T. A. J., Vincent, L. A., Roberts, T. M., & Sturgill, T. W. (1992) *Science 257,* 1404−1407.

Fenn, J. B., Mann, M., Meng, C. K., Wong, S. F., & Whitehouse, C. M. (1989) *Science 246,* 64−71.

Fukasawa, K., Murakami, M. S., Blair, D. G., Kuriyama, R., Hunt, T., Fischinger, P., & Vande Woude, G. F. (1994) *Cell Growth Diff.* (in press.)

Gardner, A. M., Vaillancourt, R. R., Lange-Carter, C. A., & Johnson, G. L. (1994) *Mol. Biol. Cell 5,* 193−201.

Gibson, B. W., & Cohen, P. (1990) *Methods Enzymol. 193,* 480−501.

Gotoh, Y., Matsuda, S., Takenaka, K., Hattori, S., Iwamatsu, A., Ishikawa, M., Kosoko, H., & Nishida, E. (1994) *Oncogene 9,* 1891−1898.

Hanks, S. K., & Quinn, A. M. (1991) *Methods Enzymol. 200,* 38−62.

Haystead, T. A. J., Dent, P., Wu, J., Haystead, C. M. M., & Sturgill, T. W. (1992) *FEBS Lett. 306,* 17−22.

Her, J. H., Lakhani, S., Zu, K., Vila, J., Dent, P., Sturgill, T. W., & Weber, M. J. (1993) *Biochem. J. 296,* 25−31.

Howe, L. R., Leevers, S. J., Gomez, N., Nakielny, S., Cohen, P., & Marshall, C. J. (1992) *Cell 71,* 335−342.

Huang, W., & Erikson, R. L. (1994) *Proc. Natl. Acad. Sci. U.S.A. 91,* 8960−8963.

Kamps, M. P., & Sefton, B. M. (1989) *Anal. Biochem. 176,* 22−27.

Katta, V., Chowdhury, S. K., & Chait, B. T. (1991) *Anal. Chem. 63,* 174−178.

Kyriakis, J. M., App, H., Zhang, X., Banerjee, P., Brautigan, D. L., Rapp, U. R., & Avruch, J. (1992) *Nature 358,* 417−421.

Lange-Carter, C. A., Pleiman, C. M., Gardner, A. M., Blumer, K. J., & Johnson, G. L. (1993) *Science 260,* 315−319.

Mansour, S. J., Matten, W. T., Hermann, A. S., Candia, J. M., Rong, S., Fukasawa, K., Vande Woude, G. F., & Ahn, N. G. (1994a) *Science 265,* 966−970.

Mansour, S. J., Resing, K. A., Candia, J. M., Hermann, A. S., Gloor, J. W., Herskind, K. R., Wartmann, M., Davis, R. J., & Ahn, N. G. (1994b) *J. Biochem. 116,* 304−314.

Matsuda, S., Kosako, H., Takenaka, K., Moriyama, K., Sakai, H., Akiyama, T., Gotoh, Y., & Nishida, E. (1992) *EMBO J. 11,* 973−982.

McLafferty, F. W. (Ed.) (1983) *Tandem Mass Spectrometry,* John Wiley & Sons, New York.

Nebreda, A., & Hunt, T. (1993) *EMBO J. 12,* 1979−1986.

Neiman, A. M., & Herskowitz, I. (1994) *Proc. Natl. Acad. Sci. U.S.A. 91,* 3398−3402.

Neiman, A. M., Stevenson, B. J., Xu, H.-P., Sprague, G. F., Herskowitz, I., Wigler, M., & Marcus, S. (1993) *Mol. Biol. Cell 4,* 107−120.

Nishida, E., & Gotoh, Y. (1993) *Trends Biochem. Sci. 18,* 128−131.

Palczewski, K., Buczylko, J., VanHooser, P., Carr, S. A., Huddleston, J. J., & Crabb, J. W. (1992) *J. Biol. Chem. 267,* 18991−18998.

Payne, D. M., Rossomando, A. J., Martino, O. P., Erickson, A. K., Her, J., Shabanowitz, J., Hunt, D. F., Weber, M. J., & Sturgill, T. W. (1991) *EMBO J. 10,* 885−892.

Posada, J., & Cooper J. (1992) *Science 255,* 212−215.

Posada, J., Yew, N., Ahn, N. G., Vande Woude, G. F., & Cooper, J. A. (1993) *Mol. Cell. Biol. 13,* 2546−2553.

Resing, K. A., Johnson, R. S., & Walsh, K. A. (1993) *Biochemistry 32,* 10036−10045.

Robbins, D. J., & Cobb, M. H. (1992) *Mol. Biol. Cell 3,* 299−308.

Robbins, D. J., Zhen, E., Owaki, H., Vanderbilt, C. A., Ebert, D., Geppert, T. D., & Cobb, M. H. (1993) *J. Biol. Chem. 268,* 5097−5106.

Rossomando, A. J., Wu, J., Hanspeter, M., Shabanowitz, J., Hunt, D. F., Weber, M. J., & Sturgill, T. W. (1992) *Proc. Natl. Acad. Sci. U.S.A. 89,* 5779−5783.

Saito, Y., Gomez, N., Campbell, D. G., Ashworth, A., Marshall, C. J., & Cohen, P. (1994) *FEBS Lett. 341,* 119−124.

Seger, R., Ahn, N. G., Posada, J., Munar, E. S., Jensen, A. M., Cooper, J. A., Cobb, M. H., & Krebs, E. G. (1992a) *J. Biol. Chem. 267,* 14373−14381.

Seger, R., Seger, D., Lozeman, F. J., Ahn, N. G., Graves, L. M., Campbell, J. S., Ericsson, L., Harrylock, M., Jensen, A. M., & Krebs, E. G. (1992b) *J. Biol. Chem. 267,* 25628−25631.

Shibuya, E. K., & Ruderman, J. V. (1993) *Mol. Biol. Cell 4,* 781−790.

Yan, M., & Templeton, D. J. (1994) *J. Biol. Chem. 269,* 19067−19073.

Zhang, F., Strand, A., Robbins, D., Cobb, M. H., Goldsmith, E. J. (1994) *Nature 367,* 704−711.

Zheng, C. F., & Guan, K. L. (1994) *EMBO J. 13,* 1123−1131.

Zhou, Z., Gartner, A., Cade, R., Ammerer, G., & Errede, B. (1993) *Mol. Cell. Biol. 13,* 2069−2080.

BI9421679